

## Supplementary Information (SI) for “Synthesis of MXene/Carbon Composites via Controlled Etch-ing of $\text{Ti}_3\text{SiC}_2$ in gaseous etchant $\text{CCl}_4$ ”

### 1. Experimental device

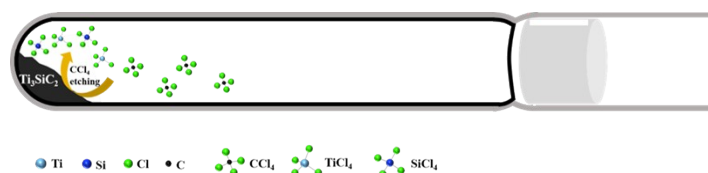


Figure S1 Experimental device (Taking  $\text{CCl}_4$  etching  $\text{Ti}_3\text{SiC}_2$  as an example)

### 2. Thermodynamic feasibility calculation

The thermodynamic feasibility of these reactions at various temperatures was assessed by calculating the Gibbs free energy using data from the NIST-JANAF Thermochemical Tables. In general, the M–X bonds in the MAX phase are characterized by strong covalent and ionic bonding, whereas the M–A bonds primarily consist of weaker metallic bonding.<sup>1,2</sup> Based on these distinctions, the calculation assumes that the  $\text{M}_{n+1}\text{X}_n$  layer does not contribute to the reaction, with the A-site elements of the MAX phase being the first to react with the etchant.<sup>3,4</sup> Under thermal conditions,  $\text{Ti}_3\text{C}_2$  MXene transforms into TiC, indicating that TiC represents the most stable structure of  $\text{Ti}_3\text{C}_2$  MXene.<sup>5</sup> The calculation results demonstrate that the  $\Delta G$  of equation S2 is less than 0, suggesting that the reaction is thermodynamically favorable. Consequently,  $\text{Ti}_3\text{C}_2$  MXene, being less stable than TiC, exhibits a greater tendency to react. In summary, the  $\Delta G$  values for both equations S1 and S2 are negative, indicating that the reactions are thermodynamically feasible.

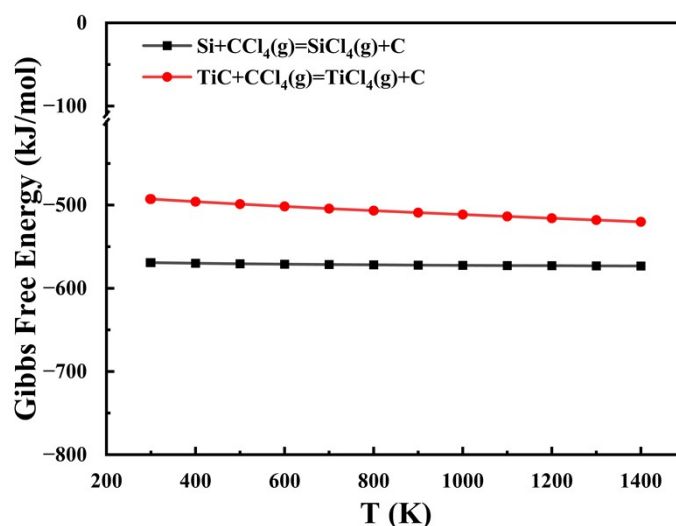
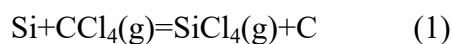


Figure S2 The Gibbs free energy of equations 1 and 2

### 3. The effect of reaction time on responses

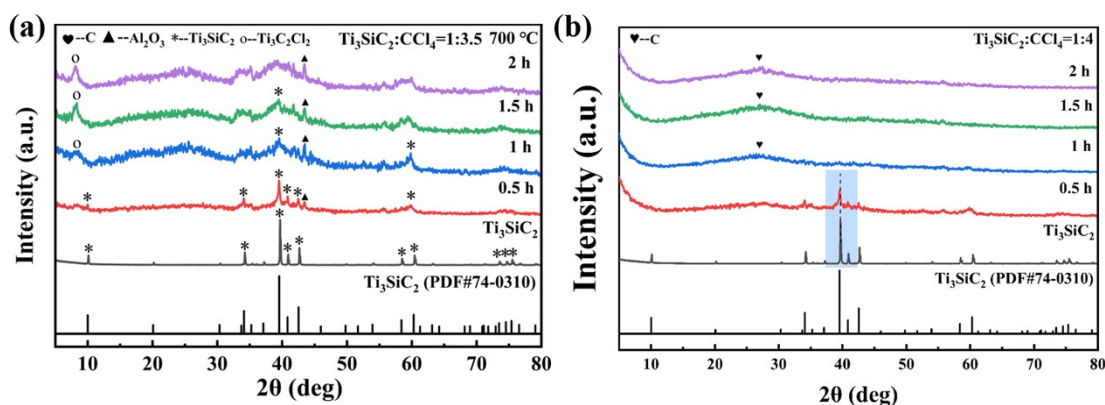


Figure S3 The XRD patterns of (a)  $\text{Ti}_3\text{SiC}_2:\text{CCl}_4 = 1:3.5$  molar ratio and (b)  $\text{Ti}_3\text{SiC}_2:\text{CCl}_4 = 1:4$  molar ratio under different reaction times.

From Figure S3 (a), it can be observed that  $\text{Ti}_3\text{SiC}_2$  gradually transforms into MXene as the reaction time increases, and it completely converts to MXene after two hours. Therefore, we set the reaction time to two hours. According to Figure S3 (b), when the reaction time is 1 hour or more,  $\text{CCl}_4$  can completely etch  $\text{Ti}_3\text{SiC}_2$  to form CDC, which indicates a possibility that increasing  $\text{CCl}_4$  may shorten the reaction time.

### 4. Analysis of gaseous products using chromatography-mass spectrometry

Gas chromatography–mass spectrometry (GC-MS) was used to analyze the gas products generated under different reaction conditions. Chloroform was used as the solvent to ensure complete dissolution of the gas-phase products, such as  $\text{SiCl}_4$  and  $\text{TiCl}_4$ , which we anticipated. The results are presented in Figure S4 and Table S1. As shown in Table S1, the main products separated by gas chromatography were  $\text{SiCl}_4$  and  $\text{HCl}$ . Other compounds may have resulted from minor contamination, such as during the carbon plating of the silica ampoules or the reaction of active gas-phase products with substances like air or water during sample preparation. The detection of  $\text{SiCl}_4$  confirms the process described by Equation 1. Based on the observation of thick smoke escaping after breaking the silica ampoules and the detection of  $\text{HCl}$  by gas chromatography, we infer that  $\text{TiCl}_4$  is likely formed during the reaction.  $\text{TiCl}_4$  reacts easily with water in the air upon exposure, producing  $\text{TiO}_2$  and  $\text{HCl}$ . Although there is no direct evidence for the existence of  $\text{TiCl}_4$ , we believe its formation is supported by the experimental phenomena and the detection of  $\text{HCl}$ . With advancements in analytical techniques and improvements in experimental setups, *in situ* analysis of such reactions may become possible in the future.

In Table S1, peaks marked with '\*' correspond to chloroform used as the solvent. Some substances in Table S1 were separated within very close retention times, and the mass spectrometry identified them as the same substance due to the presence of isomers. Since these are not the main components and do not affect the experimental conclusions, further investigation into these substances was not pursued. Furthermore,  $\text{CCl}_4$  was not detected in the mass spectrometry, which indicates that a complete reaction occurred under these conditions.

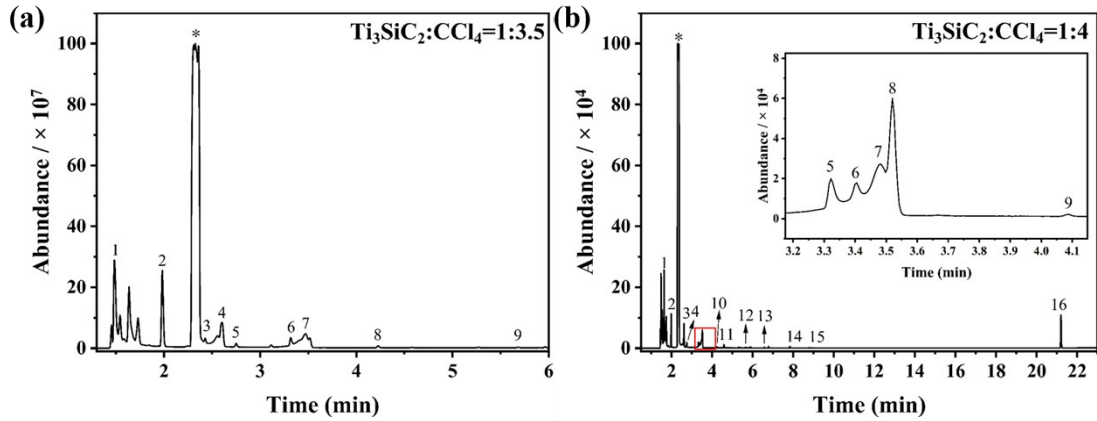


**Figure S4** The chromatograms of gas products in the reaction process with (a)  $\text{Ti}_3\text{SiC}_2:\text{CCl}_4 = 1:3.5$  molar ratio and (b)  $\text{Ti}_3\text{SiC}_2:\text{CCl}_4 = 1:4$  molar ratio

**Table S1** Qualitative and relative content analysis results of gas phase products during the reaction process with  $\text{Ti}_3\text{SiC}_2:\text{CCl}_4 = 1:3.5 / 1:4$  molar ratio

Sample	No.	Retention time	Odorant	Relative concentration (%)
$\text{Ti}_3\text{SiC}_2:\text{CCl}_4=1:3.5$	1	1.482	Hydrogen chloride	36.27
	2	1.983	Silicon tetrachloride	24.32
	3	2.556	Silane, methoxy-trichloro-	10.78
	4	2.600	Silane, methoxy-trichloro-	14.25
	5	2.749	Butane, 2-chloro-2-methyl-	1.05
	6	3.316	Silane, triethoxymethyl-	2.30
	7	3.471	1,1,3,3-Tetramethyl-3-(1-methylpropoxy)disloxan-1-ol	10.01
	8	4.225	Silane, diethoxydimethyl-	0.72
	9	5.685	Disiloxane,1,3-dichloro-1,1,3,3-tetramethyl-	0.31
$\text{Ti}_3\text{SiC}_2:\text{CCl}_4=1:4$	1	1.482	Hydrogen chloride	31.25
	2	1.983	Silicon tetrachloride	11.98
	3	2.617	Silane, methoxy-trichloro-	11.19
	4	2.755	Butane, 2-chloro-2-methyl-	1.71
	5	3.322	Silane, methylethoxyisopropoxymethoxy-	3.22
	6	3.405	Silane, dichloro-bis(methoxy)-	3.34
	7	3.482	1,1,3,3-Tetramethyl-3-(1-methylpropoxy)disloxan-1-ol	6.26
	8	3.520	Silane, chloro-tris(methoxy)-	7.78
	9	4.088	Silane, diethoxydimethyl-	0.13
	10	4.231	Silane, diethoxydimethyl-	0.57
	11	4.583	3,5-Disilaheptane, 3,3,5,5-tetramethyl-	1.50
	12	5.658	Phenyldimethylmethoxysilane	0.32
	13	6.787	Silane, diethoxydimethoxy-	0.73
	14	7.839	Silane, triethoxymethoxy-	0.78
	15	8.798	Tetraethyl silicate	0.25
	16	21.198	Benzene, hexachloro-	18.62

## 5. The etching effect of $\text{CCl}_4$ on other MAX phases ( $\text{Ti}_3\text{AlC}_2$ , $\text{Ti}_2\text{AlC}$ and $\text{Nb}_2\text{AlC}$ )

Figure S5-S7 show the etching effect of  $\text{CCl}_4$  on  $\text{Ti}_3\text{AlC}_2$ ,  $\text{Ti}_2\text{AlC}$  and  $\text{Nb}_2\text{AlC}$ , which can etch the above MAX phase into the corresponding MXene.<sup>6, 7</sup> This confirms that  $\text{CCl}_4$  is not only capable of etching  $\text{Ti}_3\text{SiC}_2$ , which is considered difficult to etch, but also shows a significant etching effect on other MAX phases, reflecting the universality of  $\text{CCl}_4$  as an effective etchant.

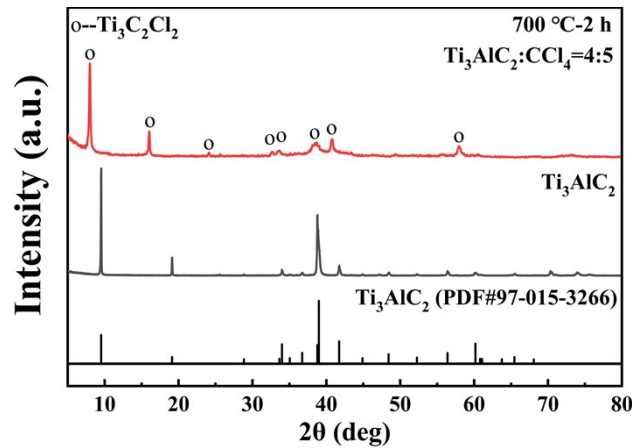


Figure S5 The etching effect of  $\text{CCl}_4$  on  $\text{Ti}_3\text{AlC}_2$

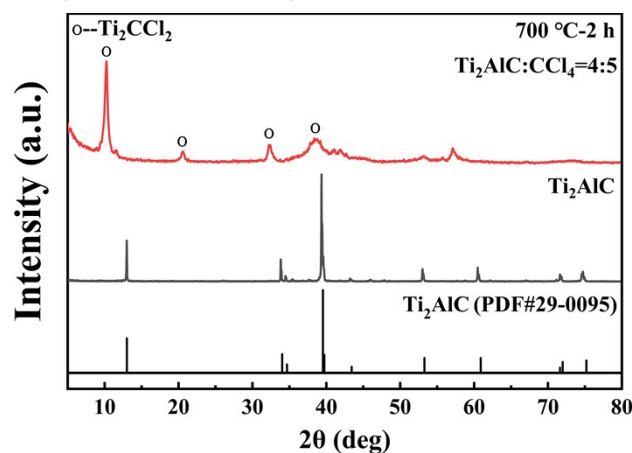


Figure S6 The etching effect of  $\text{CCl}_4$  on  $\text{Ti}_2\text{AlC}$

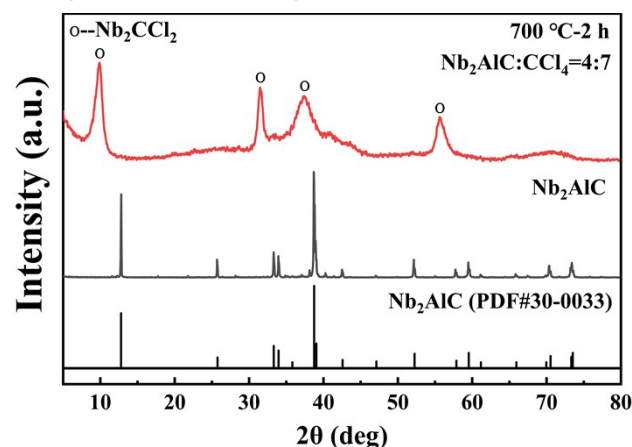


Figure S7 The etching effect of  $\text{CCl}_4$  on  $\text{Nb}_2\text{AlC}$

## 6. On the treatment and recovery of gaseous products

$\text{CCl}_4$ , as well as the  $\text{SiCl}_4$  and  $\text{TiCl}_4$  generated during the experiment, may contribute to environmental pollution. Referring to the properties and industrial

treatment methods of  $\text{CCl}_4$ ,  $\text{SiCl}_4$ , and  $\text{TiCl}_4$ , these substances, with their low melting and boiling points, can be readily separated by heating, allowing the gaseous products to be isolated from the solid products. The gaseous products are then condensed and collected, followed by fractionation for separation, facilitating the recovery and reuse of the products. If elimination is necessary, the generated gas products will first be introduced into ethanol for absorption. The ethanol will then be filtered and treated with an alkaline solution to ensure safe and harmless handling of the products. Due to the small scale of this experiment,  $\text{CCl}_4$  was removed through the addition of ethanol and subsequent filtration, which also eliminated the  $\text{SiCl}_4$  and  $\text{TiCl}_4$  generated during the process.

#### Reference:

1. M. Naguib, M. Kurtoglu, V. Presser, J. Lu, J. Niu, M. Heon, L. Hultman, Y. Gogotsi and M. W. Barsoum, *Advanced Materials*, 2011, **23**, 4248-4253.
2. M. Magnuson and M. Mattesini, *Thin Solid Films*, 2017, **621**, 108-130.
3. M. Li, J. Lu, K. Luo, Y. Li, K. Chang, K. Chen, J. Zhou, J. Rosen, L. Hultman, P. Eklund, P. Persson, S. Du, Z. Chai, Z. Huang and Q. Huang, *J Am Chem Soc*, 2019, **141**, 4730-4737.
4. Y. Li, H. Shao, Z. Lin, J. Lu, L. Liu, B. Duployer, P. O. Å. Persson, P. Eklund, L. Hultman, M. Li, K. Chen, X.-H. Zha, S. Du, P. Rozier, Z. Chai, E. Raymundo-Piñero, P.-L. Taberna, P. Simon and Q. Huang, *Nature Materials*, 2020, **19**, 894-899.
5. S. Hu, S. Li, W. Xu, J. Zhang, Y. Zhou and Z. Cheng, *Ceramics International*, 2019, **45**, 19902-19909.
6. V. Kamysbayev, A. S. Filatov, H. Hu, X. Rui, F. Lagunas, D. Wang, R. F. Klie and D. V. Talapin, *Science*, 2020, **369**, 979-983.
7. M. Xiang, Z. Shen, J. Zheng, M. Song, Q. He, Y. Yang, J. Zhu, Y. Geng, F. Yue, Q. Dong, Y. Ge, R. Wang, J. Wei, W. Wang, H. Huang, H. Zhang, Q. Zhu and C. J. Zhang, *The Innovation*, 2024, **5**, 100540.